JOURNAL OF THE ROYAL SOCIETY Interface

rsif.royalsocietypublishing.org

Research

Cite this article: Lu Q, Danner E, Waite JH, Israelachvili JN, Zeng H, Hwang DS. 2012 Adhesion of mussel foot proteins to different substrate surfaces. J R Soc Interface 10: 20120759.
http://dx.doi.org/10.1098/rsif.2012.0759

Received: 19 September 2012
Accepted: 1 November 2012

Subject Areas:
biomechanics, biochemistry, bioengineering

Keywords:
mussel foot proteins, coatings and adhesives, molecular interactions, surface forces, bioadhesion

Authors for correspondence:
Dong Soo Hwang
e-mail: dshwang@postech.ac.kr
Hongbo Zeng
e-mail: hongbo.zeng@ualberta.ca

Electronic supplementary material is available at http://dx.doi.org/10.1098/rsif.2012.0759 or via http://rsif.royalsocietypublishing.org.

Royal Society Publishing
Informing the science of the future

Adhesion of mussel foot proteins to different substrate surfaces

Qingye Lu[1], Eric Danner[4], J. Herbert Waite[3,4], Jacob N. Israelachvili[2,3], Hongbo Zeng[1] and Dong Soo Hwang[5]

[1]Chemical and Materials Engineering, University of Alberta, Edmonton, Alberta, Canada T6G 2V4
[2]Department of Chemical Engineering, [3]Materials Research Laboratory, and [4]Department of Molecular, Cell and Developmental Biology, University of California, Santa Barbara, CA 93106, USA
[5]POSTECH Ocean Science and Technology Institute, School of Environmental Science and Engineering, Pohang University of Science and Technology, Hyoja-Dong, Nam-Gu, Pohang, Gyeongbuk 790784, Korea

Mussel foot proteins (mfps) have been investigated as a source of inspiration for the design of underwater coatings and adhesives. Recent analysis of various mfps by a surface forces apparatus (SFA) revealed that mfp-1 functions as a coating, whereas mfp-3 and mfp-5 resemble adhesive primers on mica surfaces. To further refine and elaborate the surface properties of mfps, the force–distance profiles of the interactions between thin mfp (i.e. mfp-1, mfp-3 or mfp-5) films and four different surface chemistries, namely mica, silicon dioxide, polymethylmethacrylate and polystyrene, were measured by an SFA. The results indicate that the adhesion was exquisitely dependent on the mfp tested, the substrate surface chemistry and the contact time. Such studies are essential for understanding the adhesive versatility of mfps and related/similar adhesion proteins, and for translating this versatility into a new generation of coatings and (including *in vivo*) adhesive materials.

1. Introduction

Mussels survive in turbulent ocean environments by robust attachment to wave- and wind-swept substrata using a proteinaceous holdfast or byssus. Each byssus consists of specially assembled fibre, adhesive and coating proteins that cooperatively provide tenacity despite cyclic mechanical, chemical and biological stresses that arise from changes in the salinity, temperature, exposure and immersion, flow and microbial density in seawater. There are interesting parallels between the capacity of the byssus to maintain its integrity in the sea and the desirable properties for a biomaterial, such as a dental or tissue adhesive, introduced into a variety of physiological environments in the human body and submitted to flowing body fluids, degradation by endogenous enzymes and immunogenic attacks. Therefore, understanding the adhesion mechanism of mussel adhesive and coating proteins is surprisingly relevant to the design and development of biomedical adhesive and coating materials [1–6]. Mussels are also able to form underwater bonds to various substrates, such as glass, plastic and metal oxides. Indeed, the mechanism of water-resistant adhesion and coating to various substrates has attracted significant interests for potential use in biomedical applications. Understanding the interaction between individual mussel foot proteins (mfps) and different substrates will provide useful insights for the design of novel medical adhesives and coating materials.

Mfps from the *Mytilus* genus, comprising more than eight different proteins, are secreted from the mussel foot and responsible for adhesion and coating of the mussel byssus. All these proteins contain the post-translationally modified amino acid 3,4-dihydroxyphenyl-L-alanine (DOPA), derived from hydroxylation of tyrosine residue, and they are positively charged polyelectrolytes with high isoelectric points (pI ~ 10). It was reported that DOPA enables mfps to interact with various substrates under water, and that oxidative conversion of DOPA to *o*-quinone significantly reduces adhesion of mfps [7–10] except stainless steel [11]. Mfp-1 has been speculated as a coating based on

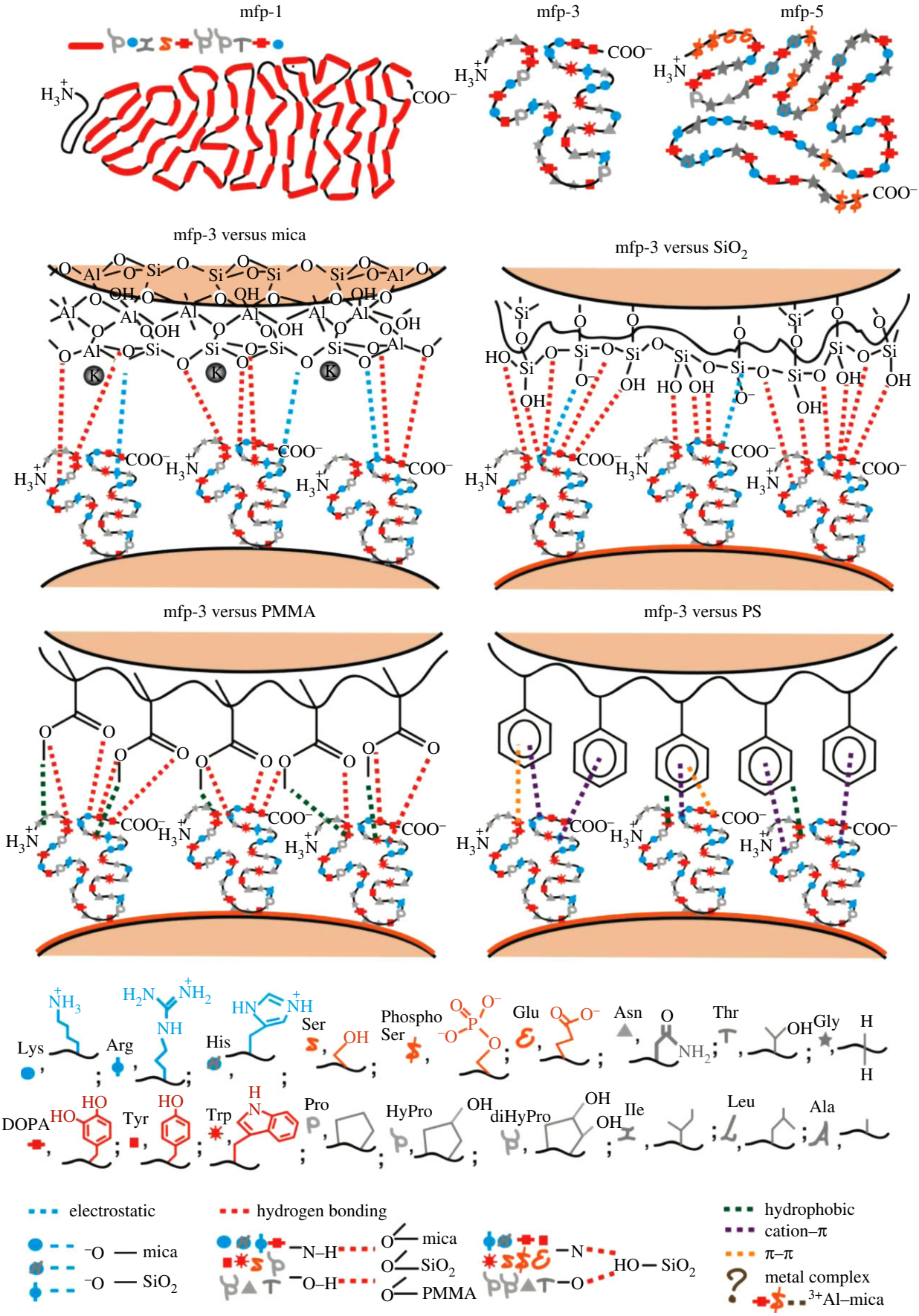

Figure 1. A schematic of the chemical structures of three mfps and four substrate surfaces, highlighting likely interactions between the mfps (mfp-3 as an example) and the different surface types. The red rod in mfp-1 stands for the decapeptide.

its outermost distribution in the byssus, whereas mfp-3 and mfp-5 were speculated to be adhesive primers owing to their distribution at interfaces between adhesive plaque and substratum [5,8,12].

Mfp-1 is composed of 64 tandem repeats of a decapeptide [Pro-Lys-Ile-Ser-DOPA-diHyp-Hyp-Thr-DOPA-Lys] (the red-rod schematic in figure 1 stands for the decapeptide), in which HyP, diHyP and DOPA denote *trans*-4-hydroxyproline,

Table 1. Comparison of the protein properties.

			mfp-1	mfp-3	mfp-5
mass (kDa)			92.0	5.3	9.5
pI			10.3	10.1	8.3
post-translational modifications	hydroxylation (Hy)	DOPA	13.0	19.0	25.5
		diHyP	5.9	0	0
		HyP	18.2	0	0
		HyArg	0	1.0	0.5
		total	37.1	20.0	26.0
	Phosphorylation		0	0	9.4
basic amino acids	Lys		19.4	15.0	19.5
	Arg, HyArg		1.0	9.5	3.1
	His		0.4	1.0	6.5
	total		20.8	25.5	29.1
amino acids favouring protein flexibility [16,17]	Gly, Thr, Arg, Ser, Gln, Asn, Asp, Pro, Glu, Lys (mol%)		50.4	70.0	61.1
hydrophobicity	aromatic (mol%, Phe, Tyr, Trp, DOPA)		19.2	26.5	26.2
	aliphatic (mol%, Val, Leu, Ile, Pro, Met)		9.4	9.0	2.9
	total		28.6	35.5	29.1

trans-2, 3, *cis*-3, 4-dihydroxyproline and DOPA, respectively [13]. Mfp-3 are interfacial adhesive proteins composed of more than 35 variants. Protein masses for the entire mfp-3 family range between 5 and 7.5 kDa. All variants contain 4-hydroxyarginines (HyArg) and approximately 20 mol% of DOPA as post-translationally modified amino acids [14]. Mfp-5 is also an interfacial adhesive protein containing o-phospho-serine as a unique post-translationally modified amino acid. Mfp-5 has the highest DOPA (approx. 25.5 mol%) among all plaque proteins, i.e. with around one in every four residues [14]. The detailed comparison of the three kinds of proteins used in the study is shown in table 1 [13–15].

The interfacial properties of mfps were here investigated by a surface forces apparatus (SFA) [4,9,10,12,18–23], which has been widely used to measure the intermolecular and surface forces in various biological and non-biological systems with nanonewton force sensitivity and less than 0.1 nm distance resolution [4,24–29]. To date, the comparison of the molecular interaction forces between the different mfps (mfp-1, mfp-3, mfp-5, especially mfp-5) and various surface chemistries have not been systematically studied. In the present work, the interaction force–distance profiles were directly measured between mfp-1, mfp-3 or mfp-5 and various substrates—mica, silicon dioxide (SiO_2), polymethylmethacrylate (PMMA), polystyrene (PS)—using an SFA in aqueous solutions to better understand the underwater adhesion and coating mechanisms of mfps.

2. Material and experimental methods

2.1. Protein purification from mussel feet

Mussels (*Mytilus californianus*) were collected for the purification of mfp-1 and mfp-3 from Goleta Pier in Goleta, CA, USA. The feet of mussel were carefully dissected, depigmented by scraping with a razor blade and stored at −80°C before use. Blue mussel (*Mytilus edulis* L.) feet for the purification of mfp-5 were obtained in flash-frozen 500 g lots from the North East Transport of Union, Maine. Mfp-1, mfp-3 and mfp-5 were purified from frozen mussel feet according to published procedures [15,18,30]. Sample purity was assessed by acid urea poly-acrylamide gel electrophoresis, amino acid analysis and MALDI-TOF mass spectrometry. The mole % DOPA in purified mfp-1, mfp-3 and mfp-5 was approximately 13, approximately 23 and 28 mol%, respectively, determined by amino acid analysis after a 1 h hydrolysis in 6 N HCl at 158°C. Purified samples were freeze-dried and resuspended in 50 mM acetic acid (0.1 mg ml^{-1}) and thereafter divided into convenient aliquot volumes for storage in vials at −80°C prior to testing. Low pH and protection from light are necessary to reduce DOPA losses during handling and storage [4,18]. All aliquots were used within one month or otherwise discarded because protein adhesive quality falls off abruptly during long-term storage [10]. Milli-Q water (Millipore, Mississauga, ON, Canada) was used for all glassware cleaning and solution preparation.

2.2. Chemicals

The buffer for SFA measurements consisted of 0.1 M acetic acid (HAc) (Fisher Scientific, Ottawa, ON, Canada), and sodium acetate (NaAc) (Merck& Co. Limited, Montreal, QC, Canada), and 0.25 M potassium nitrate (KNO_3) (MP Biomedicals, Solon, OH, USA) at pH 5.5. Aqueous solutions were prepared in Milli-Q water (Millipore) and filtered through 0.2 µm filters (Nalgene, Rochester, NY, USA). PS (MW 10^6, M_W/M_n 1.10) was obtained from Polysciences (Warrington, PA, USA). PMMA (MW 35 kDa) was purchased

from Scientific Polymer Products, Inc (Ontario, NY, USA). PS and PMMA were dissolved in toluene (Fisher Scientific) and the solutions were filtered through 0.2 µm PTFE filters (Fisher Scientific) before use.

2.3. Preparation and characterization of substrate surfaces

Four different substrate surfaces were prepared for the SFA measurements: mica, mica-supported SiO_2, mica-supported PMMA and mica-supported PS (figure 1). On the basis of a previously reported procedure [18,26,29], two thin and back-silvered mica sheets (1–5 µm thick) were glued separately onto cylindrical silica discs (radius $R = 2$ cm) and the exposed mica surfaces were directly used or further coated with different chemicals (i.e. SiO_2, PMMA and PS) as follows. Thin layers of SiO_2 (approx. 15 nm) were deposited onto mica by E-beam evaporation (PVD-75, Kurt J. Lesker) at approximately 0.05 nm s^{-1} with 1.5×10^{-5} Torr of O_2 and $(2–8) \times 10^{-6}$ Torr of H_2O. Thin layers of PS or PMMA were coated onto mica by spin-coating using 0.5 wt% PS or PMMA solution in toluene and vacuum dried at 23°C overnight.

The surface roughness of the different substrates was characterized by atomic force microscopy (AFM, Agilent Technologies 5500, Santa Barbara, CA, USA). The surfaces were imaged with a silicon tip (AppNANO, ACT-200, Si, N-type, tip radius < 10 nm, resonant frequency 318 kHz) operating in the tapping mode in air. Water contact angle measurements were performed using a contact angle goniometer (KRUSS DSA 10, Germany).

2.4. SFA force measurements

The force measurements between proteins and substrate surfaces were performed using an SFA (Surforce LLC, Santa Barbara, CA, USA) in a configuration reported previously [4,10,12,18,26,28]. A protein film was adsorbed onto each type of substrate surface according to a recent procedure [4]. Briefly, for each SFA measurement, 50 µl of the protein solution (10 µg ml^{-1} in 0.1 M NaAc, 0.25 M KNO_3, pH 5.5) were placed onto the substrate and incubated for 10 min in a chamber saturated with water vapour. Then the surface was rinsed with pure buffer and mounted in the SFA chamber together with another bare substrate surface in a cross-cylinder configuration. The interaction forces F between the two surfaces in pH 5.5 buffer were measured as a function of the absolute surface separation distance D as determined using multiple beam interferometry.

During a typical SFA force measurement, the two surfaces (e.g. an mfp film and a substrate surface) were first brought towards each other to reach a 'hard wall contact' and kept in contact for a certain time, followed by separation. The 'hard wall' distance is defined as the confined distance between the two surfaces, which did not appear to significantly change on increasing the normal (compressive) load or pressure. If two surfaces attract one another, an adhesion force F_{ad} is measured during separation, and the surfaces jump apart from adhesive contact when the tensile load exceeds F_{ad}. The adhesion energy per unit area W_{ad} is related to the measured adhesion force (F_{ad}/R) by $W_{ad} = F_{ad}/1.5\pi R$ for soft deformable surfaces [20,31]. All the experiments were carried out at room temperature (23°C).

2.5. Hydropathy and flexibility analysis

To interpret SFA data, analysis of the hydropathy and chain flexibility of the mfps were performed (see the electronic supplementary material for detailed analysis methodology for hydropathy and flexibility of mfps). For the hydropathy analysis, a Hopp and Woods hydropathy analysis was used (http://web.expasy.org/protscale/) [32], which is based on Tanford and Nozaki's hydropathy measurements with DOPA [33], reflecting a high degree of post-translational modification on mfps and overall random coil conformation of mfps. Most mfps have a random conformation in aqueous solution while mfp-1 has poly-proline II domains separated by unstructured sequences [34,35]. The B-factor, also known as the atomic displacement or temperature factor determined from X-ray crystallographic studies, reflects the degree of thermal motion and static disorder of an atom in a protein crystal structure, and has been applied for predicting protein chain flexibility. Amino acids can have two types of groups, 'rigid' and 'flexible', on the basis of the B-factor that reflects the chain flexibility of 31 proteins of known three-dimensional structure in the Protein Data Bank (Brookhaven, USA) [16,17]. The portions of flexible amino acids in each mfp were calculated here to predict protein chain flexibility.

3. Results

3.1. Properties of mfps and substrate surfaces

The three kinds of mfp proteins used (mfp-1, mfp-3, mfp-5) all have high isoelectric points (pI) and exhibit a high degree of post-translational modification particularly in the hydroxylation of tyrosine to DOPA. On the other hand, they differ in molecular weights, pI values, post-translational modifications type and ratios, basic and aromatic amino acid content, and flexibility (table 1) [13–15]. Mfp-3 is a small protein (5.3 kDa) with the highest flexible amino acid residues among mfps (70 mol%) determined by B-factor that reflects the degree of flexibility of amino acids [16,35]. Mfp-3 contains 25.5 mol% basic residues and a pI of ~10.1, which has 35.5 mol% hydrophobic amino acid, including approximately 20 mol% DOPA [14]. Similar to mfp-3, mfp-5 is a small protein (9.5 kDa) with 61.1 mol% of flexible residues based on B-factor. Mfp-5 contains 29.1 mol% basic amino acids and has a pI ~ 8.3. Mfp-5 also contains negative charges (9.4 mol% phosphorylation, 2.8 mol% Glu), and has 29.1 mol% hydrophobic residues, including approximately 25.5 mol% DOPA [15]. Compared with mfp-3 and mfp-5, mfp-1 is a large protein (92.0 kDa) with much less flexibility (50.4 mol% of flexible residues). Mfp-1 contains 20.8 mol% basic amino acid and has a pI of 8.3–10.3, which has 28.6 mol% hydrophobic amino acid, including approximately 19.2 mol% DOPA. Mcfp-1 is the most rigid protein among all the mfps tested based on the B-factor and is composed of tandem repeats of stiff decapeptide units [13,36].

The four different substrate surfaces studied have wide-ranging surface chemistries (e.g. chemical compositions, structures, etc., summarized in figure 1). The hydrophobicity determined by water contact angle measurements increases in the order of mica < mica-supported SiO_2 < mica-supported PMMA < mica-supported PS, with water contact angles of less than 5°, 20°, 70° and 92°, respectively (consistent with values reported previously [28,37,38]). The root

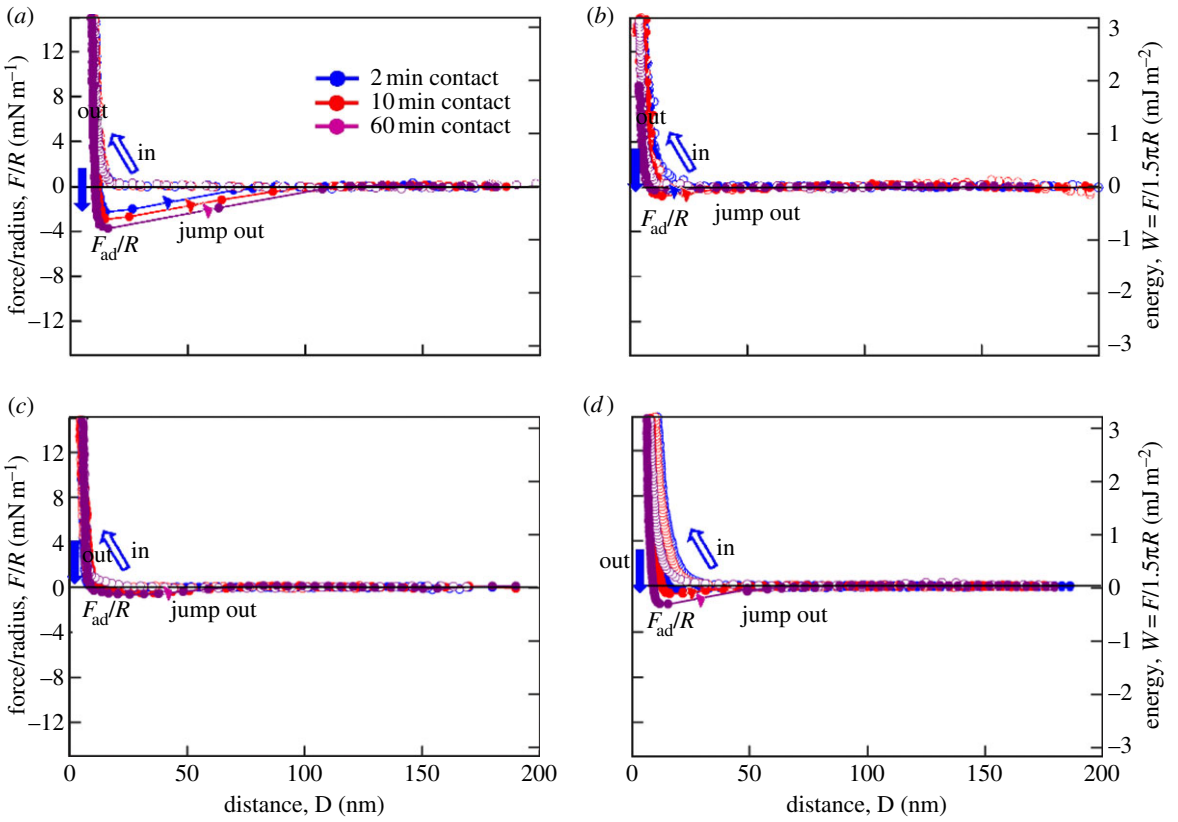

Figure 2. Mfp-1 adhesion to different substrates: (*a*) mica, (*b*) SiO_2, (*c*) PMMA and (*d*) PS with different contact times of 2 min (blue), 10 min (red) and 60 min (purple) after bringing the two surfaces into contact in buffer consisting of 0.1 M sodium acetate, 0.25 M KNO_3, pH5.5. The normalized forces, F/R, are denoted in the left ordinate, whereas the corresponding interaction energies per unit area, W (defined by $W = F/1.5\pi R$), are on the right-hand ordinate. F_{ad}/R is the normalized adhesion force.

mean square (r.m.s.) roughness determined by AFM for mica, mica-supported PMMA and PS were all less than 0.5 nm, while for mica-supported SiO_2 the r.m.s. roughness was about 1.0 nm (consistent with previous reports [28,39]).

3.2. Adhesion of mfps to mica, SiO_2, PMMA and PS

To understand the adhesive interaction mechanisms of mfps, the surface forces measurements were performed in an 'asymmetrical' configuration between three different mfps and four different opposing substrate surfaces. The adhesion results of the three mfps (mfp-1, mfp-3, mfp-5) to the four surfaces (mica, SiO_2, PMMA and PS) are presented in the following sections. The typical force–distance profiles are shown in figures 2–4, and the comparison of the interaction energies from figures 2–4 are summarized in figure 5.

The solution condition (pH 5.5 and salt concentration of 0.35 M) for the SFA measurements was chosen based on the following considerations. Seawater chemistry appears to be irrelevant to the initial deposition of adhesive proteins. Like a rubber plunger, the mussel foot positions itself snugly onto a patch of surface and imposes a new set of solution conditions in the sealed space between itself and the substratum. These conditions include an acidic pH (approx. pH 5) and low salt concentration 0.1 M [10], which are crucial adaptations, given that most mfps undergo spontaneous oxidation and are insoluble at the pH and ionic strength of seawater [10,12]. Our experiments using SFA were designed to be consistent with the known details of mussel adhesion, i.e. at a chosen pH of 5.5 with a buffer salt concentration of 0.35 M. Potassium nitrate was used in place of sodium chloride in the buffer solution to reduce the possible corrosion of the semi-reflecting silver layers under the mica substrates induced by the high concentration of chloride ions in the surface forces measurements.

3.2.1. Adhesions of mfp-1 to mica, SiO_2, PMMA and PS

Mfp-1 demonstrated weak adhesion to both hydrophobic and hydrophilic surfaces, but the adhesion clearly depends on the surface type and contact time (figure 2*a–d*).

As shown in figure 2*a*, the adhesion strengths of mfp-1 to mica were $F_{ad}/R \sim -2.3, -2.9, -3.7$ mN m^{-1} (or $W_{ad} \sim 0.5$, 0.6 and 0.8 mJ m^{-2}) for 2, 10 and 60 min contact times, respectively. These results are consistent with a recent report [18]. The adhesion of mfp-1 on SiO_2 is relatively weak, with adhesion forces of $F_{ad}/R \sim -0.5, -0.7$ and -0.4 mN m^{-1} ($W_{ad} \sim 0.10$, 0.13 and 0.07 mJ m^{-2}) for 2, 10 and 60 min contacts, respectively (figure 2*b*). The adhesion strengths of mfp-1 to PMMA were $F_{ad}/R \sim -0.05, -0.5, -0.6$ mN m^{-1} ($W_{ad} \sim 0.01$, 0.11, 0.13 mJ m^{-2}) for 2, 10 and 60 min contacts, respectively (figure 2*c*). The adhesion of mfp-1 on PS were $F_{ad}/R \sim -0.2, -0.6, -1.6$ mN m^{-1} ($W_{ad} \sim 0.06$, 0.15, 0.33 mJ m^{-2}) for 2, 10 and 60 min contacts, respectively (figure 2*d*). Overall, Mfp-1 can be readily deposited onto the four substrates using current deposition technique, and form protein layers of reproducible film thickness as determined by SFA (10 ± 0.5 nm), and the adhesion of mfp-1 with the four substrates increases in the order: mica > PS, SiO_2, PMMA (figures 2 and 5*a*).

3.2.2. Adhesion of mfp-3 to mica, SiO_2, PMMA and PS

Mfp-3 can adhere well to both hydrophilic and hydrophobic surfaces, and the adhesion strengths are again

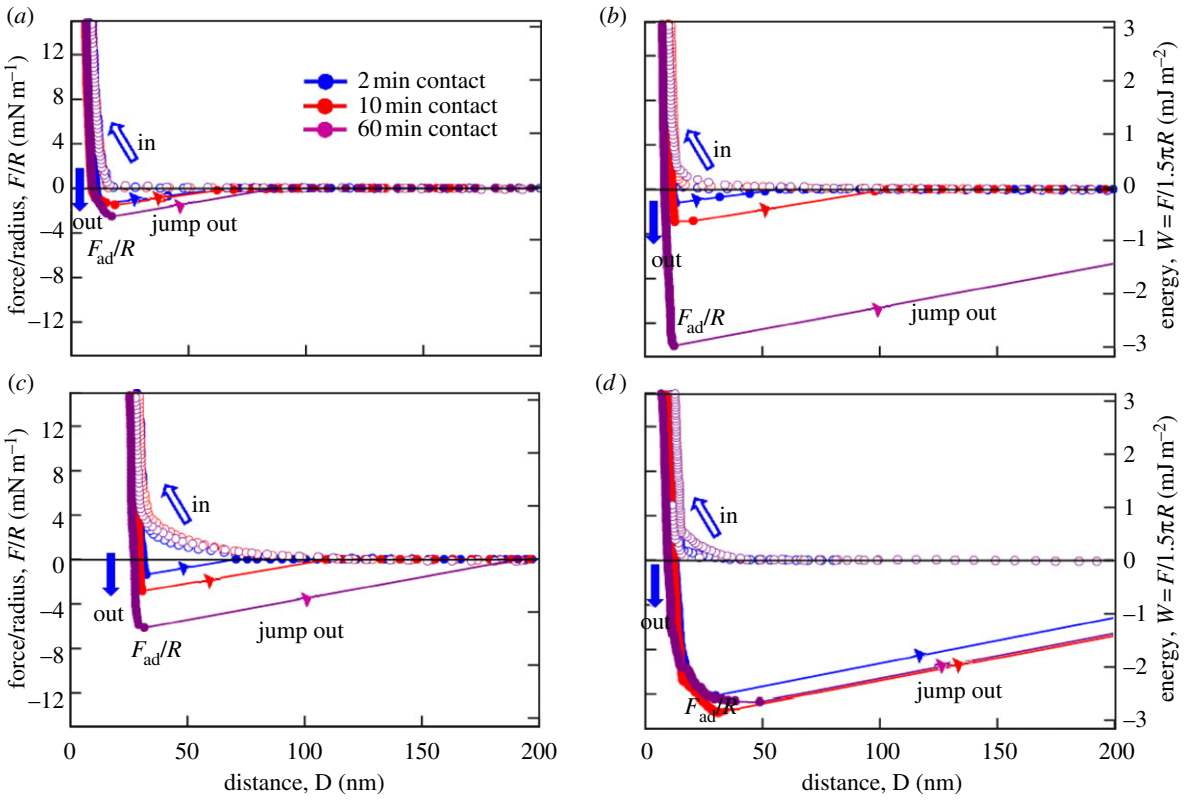

Figure 3. Mfp-3 adhesion to different substrates: (*a*) mica, (*b*) SiO_2, (*c*) PMMA and (*d*) PS with different contact times of 2 min (blue), 10 min (red) and 60 min (purple) after bringing the two surfaces in contact, in buffer consisting of 0.1 M sodium acetate, 0.25 M KNO_3, pH5.5. The normalized forces, F/R, are denoted in the left-hand ordinate, whereas the corresponding interaction energies per unit area, W (defined by $W = F/1.5\pi R$), are in the right-hand ordinate. F_{ad}/R is the normalized adhesion force.

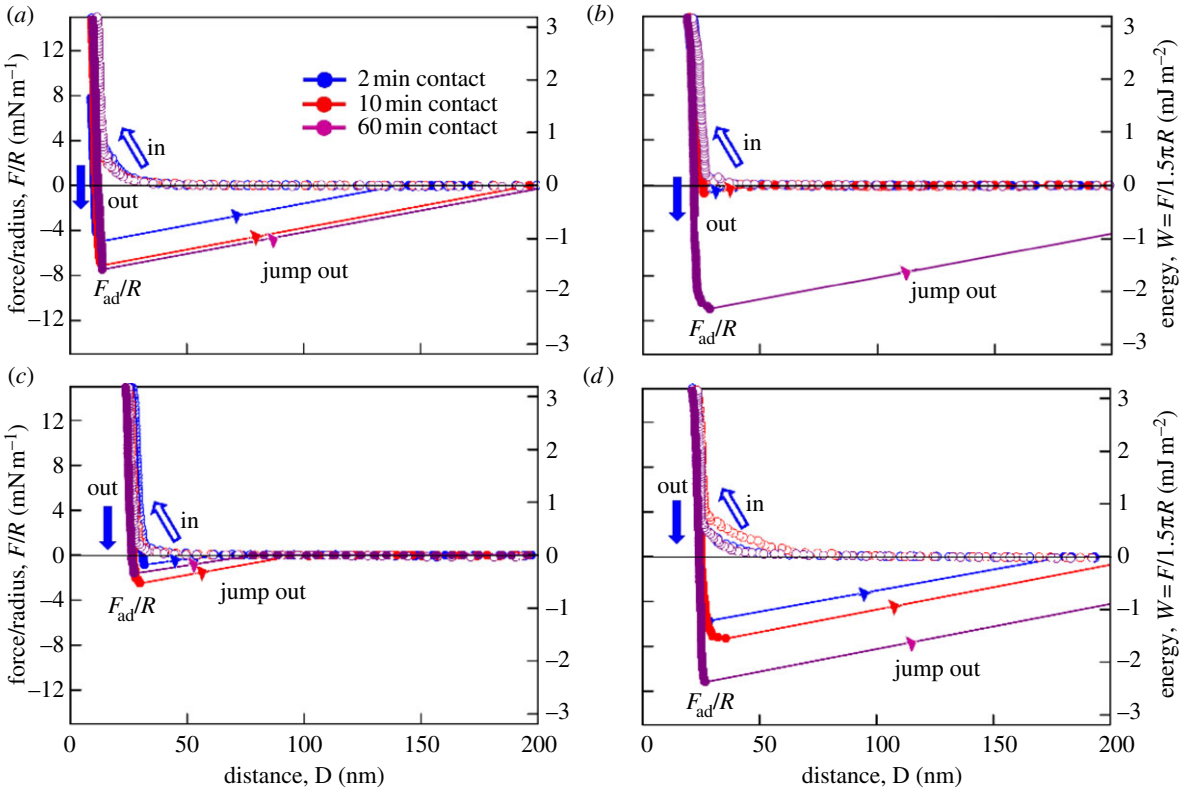

Figure 4. Mfp-5 adhesion to different substrates: (*a*) mica, (*b*) SiO_2, (*c*) PMMA and (*d*) PS with different contact times of 2 min (blue), 10 min (red) and 60 min (purple) after bringing the two surfaces into contact, in buffer consisting of 0.1 M sodium acetate, 0.25 M KNO_3, pH5.5. The normalized force, F/R, is denoted in the left-hand ordinate, whereas the corresponding interaction energy per unit area, W (defined by $W = F/1.5\pi R$), is indicated by the right-hand ordinate. F_{ad}/R is the normalized adhesion force.

substrate-dependent, as shown by the typical interaction force–distance profiles (figure 3*a–d* for mica, SiO_2, PMMA and PS, respectively). Typically, the adhesion increased with increasing contact time for almost all the cases studied for mfp-3, most probably owing to the local conformational rearrangements of the protein molecules resulting in more effective adhesive 'bonds' to the substrate surfaces. For a more flexible protein, such conformational rearrangements

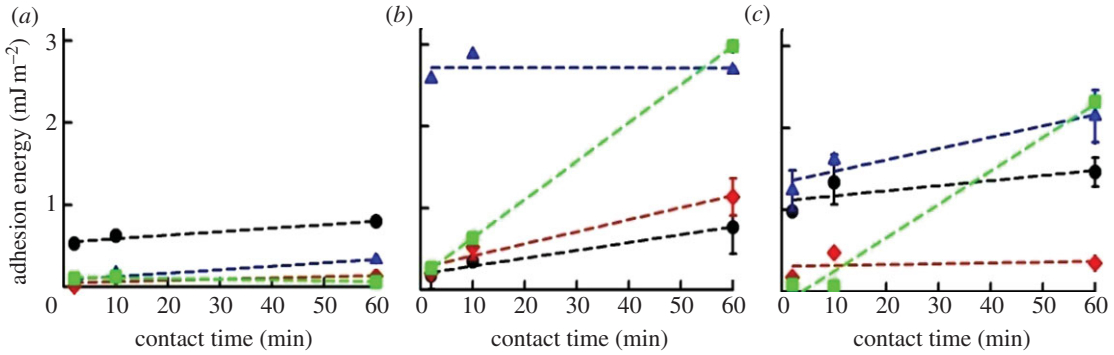

Figure 5. Relationship between adhesion energy ($W_{ad} = F_{ad}/1.5\pi R$) and contact time for (*a*) mfp-1, (*b*) mfp-3 and (*c*) mfp-5 on four different substrates: (black circles) mica, (green squares) SiO_2, (red diamonds) PMMA and (blue triangles) PS. Each point and error bar represents the mean of three force runs and its standard deviation.

can be achieved relatively easily with contact time for better adhesion. Whereas for a rigid protein, increasing contact time may not induce sufficient conformational rearrangements, and its adhesion shows relatively weak dependence on contact time, i.e. the entropic hindrance from neighbouring rigid side groups can impede the conformational arrangements of the functional groups for efficient adhesive interactions. Compared with mfp-1, mfp-3 is a smaller and more flexible protein, which makes its surface adhesion more dependent on the contact time.

The adhesion strengths of mfp-3 to mica were observed to be $F_{ad}/R \sim -1.4$, -1.5 and -3.0 mN m^{-1} ($W_{ad} \sim 0.29$, 0.31 and 0.64 mJ m^{-2}) for 2, 10 and 60 min contacts, respectively (figure 3*a*). These results are consistent with previous reports [5,12]. For mfp-3 against SiO_2, the adhesive interaction strengths were determined to be $F_{ad}/R \sim -1.2$, -3.0 and -14.1 mN m^{-1} ($W_{ad} \sim 0.26$, 0.64 and 2.99 mJ m^{-2}) for 2, 10 and 60 min contacts, respectively (figure 3*b*). The adhesion of mfp-3 to SiO_2 showed the greatest dependence on the contact time. The adhesion strengths of mfp-3 to PMMA were $F_{ad}/R \sim -0.9$, -3.0 and -6.1 mN m^{-1} ($W_{ad} \sim 0.2$, 0.64 and 1.30 mJ m^{-2}) for 2, 10 and 60 min contacts, respectively (figure 3*c*). For mfp-3 against PS, the adhesion strengths were essentially spontaneously achieved at $F_{ad}/R \sim -12.1$, -13.6 and -12.7 mN m^{-1} ($W_{ad} \sim 2.58$, 2.88 and 2.69 mJ m^{-2}) for 2, 10 and 60 min contacts, respectively (figure 3*d*). Therefore, mfp-3 protein molecules show the highest adhesion to PS among the four substrates for short contact time, and PS $\approx$ SiO_2 > PMMA > mica for long contact time (60 min). The thickness (i.e. hard wall distance) of mfp-3 layer on the four substrates was determined to be 5 ± 0.5, 6 ± 0.5, 25 ± 0.5 and 6 ± 0.5 nm for mica, SiO_2, PMMA and PS, respectively (figure 3), which indicates that the adsorption/deposition of mfp-3 to PMMA is greater than to mica, SiO_2 and PS. It should be noted that the proteins concentration and adsorption time during deposition were fixed, and the protein layer thickness was determined by repeated measurements for at least three times.

3.2.3. Adhesions of mfp-5 to mica, SiO_2, PMMA and PS

Similar to mfp-3, mfp-5 exhibits strong adhesion to both hydrophilic and hydrophobic surfaces (figure 4), and the adhesion strength depends both on surface type and contact time. Typical force–distance profiles are shown in figure 4*a–d* for mica, SiO_2, PMMA and PS. Similar to mfp-3, adhesion of mfp-5 to different substrates was found to increase with the contact time.

The adhesion of mfp-5 to mica was $F_{ad}/R \sim -4.6$, -7.2 and -7.5 mN m^{-1} ($W_{ad} \sim 0.98$, 1.53 and 1.59 mJ m^{-2}) for 2, 10 and 60 min contacts, respectively (figure 4*a*). The adhesion of mfp-5 to SiO_2 was observed to be $F_{ad}/R \sim -0.5$, -0.5 and -11.5 mN m^{-1} ($W_{ad} \sim 0.11$, 0.11 and 2.44 mJ m^{-2}) for 2, 10 and 60 min contacts, respectively (figure 4*b*). The adhesion of mfp-5 to PMMA was $F_{ad}/R \sim -1.0$, -2.9 and 2.0 mN m^{-1} ($W_{ad} \sim 0.21$, 0.62 and 0.42 mJ m^{-2}) for 2, 10 and 60 min contacts, respectively (figure 4*c*). The adhesion of mfp-5 to PS was $F_{ad}/R \sim -5.0$, -7.4 and -11.2 mN m^{-1} ($W_{ad} \sim 1.07$, 1.57 and 2.37 mJ m^{-2}) for 2, 10 and 60 min contacts, respectively (figure 4*d*). Overall, the adhesion of mfp-5 to the four different substrates follows the order PS $\approx$ mica > PMMA $\approx$ SiO_2 for short contact times (2–10 min), and PS $\approx$ SiO_2 > mica > PMMA for longer contacts (60 min; figure 5*c*). The hard wall distances for mfp-5 interaction cases of mica, SiO_2, PMMA and PS were determined to be 9 ± 0.5, 20 ± 0.5, 24 ± 0.5 and 20 ± 0.5 nm, respectively (figure 4), which indicates that the deposition of mfp-5 on SiO_2, PMMA and PS was more extensive than on mica.

4. Discussion

4.1. Effects of molecular weight and chain flexibility on the adhesion of mfps to different substrates

The molecular adhesion of mfps is generally correlated with the backbone flexibility in the proteins. It should be noted that for non-adhesive interactions, a flexible polymer in surface contact normally pays a high penalty in conformational entropy; thus its adhesion process is more entropically hindered with a more flexible backbone. For the adhesive bonding of mfps to different substrates in this study, higher chain flexibility of mfps is expected to have positive impact on the adhesion process as the local structure of the protein can better and more quickly adapt to the specific surface chemistry [40]. It should also be noted that the flexibility of surface bound polymer chains might not be the same as that in solutions, and further studies are necessary to fully resolve the relation between chain flexibility and adhesion. Chain flexibility generally decreases with increasing

molecular weight in polymers [40]. Among the three mfps studied, the molecular weights are highest for mfp-1 (92.0 kDa), then mfp-5 (9.5 kDa) and lowest for mfp-3 (5.3 kDa) (table 1). In addition, mfp-1 has the least flexibility based on the flexible amino acids composition by B-factor (50.4 mol%) compared with mfp-3 (70 mol%) and mfp-5 (61.1 mol%). A recent study based on circular dichroism (CD) and sum frequency generation (SFG) vibrational spectroscopy also revealed that mfp-3 exhibits a flexible random coil conformation in solution that easily adapts to different surface chemistries, whereas mfp-1 is mainly composed of a stiff decapeptide repeats with a poly-proline type II helix separated by flexible hinges [41–43]. Therefore, the molecular flexibility of the three mfps is mfp-3 > mfp-5 > mfp-1.

The SFA results further show that the increasing adhesion with increasing contact time (independent of substrate chemistry) followed the order mfp-3 > mfp-5 > mfp-1 (figure 5), which is also consistent with the order of molecular flexibility. The effect of chain flexibility on mfps adhesion is more significant on a rough surface such as SiO_2 where tailored smooth contact can be obtained more easily for flexible macromolecules but not for rigid macromolecules [44]; thus, a significant adhesion increase was observed for mfp-3 and mfp-5 on SiO_2 for relatively long contact times (60 min; figure 5).

4.2. Proposed adhesion mechanisms of mfps to different substrates

All three mfps showed adhesive capabilities on the four substrates of different surface chemistry. Schematics of the molecular structures and possible interaction schemes are shown in figure 1. Several interaction mechanisms can be involved during the interactions of mfps to the four surface types, including electrostatic, hydrogen bonding, hydrophobic interactions, cation–π, π–π stacking and metal-complexation (figure 1).

All three mfps have basic pIs, are positively charged at the experimental conditions (pH 5.5) and thus can attract negatively charged mica or SiO_2 surfaces under the given pH [18]. The dissolution of K^+ ions from mica and proton dissociation from mica and SiO_2 (pK_a 7.0) makes these surfaces negatively charged [45]. Under the experimental conditions (0.35 M salt), the concentrated K^+ ions in the solution can compete with the mfp molecules for adsorption sites on the substrate surfaces and thereby largely suppress the net electrostatic interaction energies [18]. Therefore, electrostatic interactions are not likely to play a major role in the adhesion of the three mfps under the experimental conditions used.

Hydrogen bonds can form between the hydroxyl or amine groups (hydrogen donors) on mfps and the oxygen atoms (hydrogen acceptors) on mica, SiO_2 and PMMA (–O–H...O, –N–H...O), and between the oxygen or nitrogen atoms on mfps and hydroxyls on SiO_2 (–O–...H–O, –N–...H–O) [7,12,18]. However, it should be noted that water molecules in the solution are also able to form hydrogen bonds with the mfps and the substrates (so-called hydration layers).

Hydrophilicity calculations on the primary amino acid sequences of the mfps with inclusion of post-translational modifications indicate that the three mfps consist predominantly of hydrophilic domains based on the Hopp and Woods hydropathy index with nine amino acids as a window (see the electronic supplementary material, figure S1). Mfp-3 and mfp-5 show strong adhesion to PS, the most hydrophobic substrate investigated. This could be due to the interaction between exposed hydrophobic amino acid residues in the mfps and PS and/or cation–π interactions or π–π stacking, as discussed in more detail below.

Cation–π and π–π interactions play important roles in the interactions of many bio-interfaces (e.g. DNA structure, protein binding). Cation–π can be formed between the positively charged amines in mfps (i.e. Lys, Arg, over approx. 20 mol%) and aromatic groups on the substrate surface, and π–π stacking can be formed between the aromatic groups on mfps (over approx. 20 mol%) and the phenyl groups on PS [18,46–49]. In terms of the interaction energy, the cation–π interaction is comparable to hydrogen bonding while π–π stacking is weaker than hydrogen bonding [46–49]. The cation–π interaction has recently been implicated in the adhesion of green mfp (pvfp-1) [46] and mcfp-1 [18], which can probably also contribute to the adhesion of mfps to PS here.

Another possible interaction involved is the complexation between metal ions and the phosphate groups present in mfp-5 (9.4 mol% phospho-Ser) [15,50,51]. Small amounts of Al are present on the surface (exposed basal plane) of mica [37] that may associate with the phospho-Ser groups in mfp-5 or DOPA groups in all three mfps at pH 5.5.

4.3. Interactions of mfps with different substrates

The possible interaction mechanisms between the mfps and the four substrates tested can now be discussed in more detail.

4.3.1. Mica

Mica is a hydrophilic mineral and its exposed surface in water solution is polysiloxane with minor replacement of Si by Al (figure 1). DOPA bidentate hydrogen bonding to mica is believed to be the main contributor for the adhesion of mfps to mica [7,9,10,18]. In particular, the distances between adjacent O atoms on mica (0.28 nm) [52] and between OH groups in DOPA (0.29 nm) almost certainly facilitates DOPA bidentate hydrogen bonding to the mica surface [7]. Previous SFA measurements demonstrated that periodate treatment (DOPA oxidation) abolishes almost all of mfp-3 adhesion and more than 75 per cent of mfp-1 adhesion on mica [9,10,18]. Thicknesses of both mfp-1 and mfp-3 films measured by the SFA increased upon DOPA oxidation. This is in stark contrast to the previously reported contraction in periodate-treated mfp-1 films analysed by surface plasmon resonance and the quartz crystal microbalance [53,54]; these authors attributed film contraction to dehydration associated with protein cross-linking. In the present case, we attribute the periodate-treated mfp-1 and mfp-3 film expansion to tautomerization of DOPA-quinone to Δ-DOPA, because it is reversible and is known to induce significant reduction in their conformational flexibility [9]. Further studies are necessary to resolve the relationships between cross-linking and tautomerization.

For mfp-1 adhesion on mica, the significant hydroxyproline content could also contribute to the adhesion [18]. Thus, the hydrogen bonding follows the order of DOPA content in mol% (table 1) [13–15], i.e. mfp-5 > mfp-3 > mfp-1. Because

of the additional contribution from hydroxyprolines in mfp-1, mfp-1 and mfp-3 may have similar hydrogen bonding strengths.

In addition to the hydrogen bonding, mica can support the formation of metal complexes via oxidized Al groups interacting with phosphoester groups in mfp-5 and DOPA groups in all mfps (figure 1). Such effects follow the order of mfp-5 > mfp-3 > mfp-1. Electrostatic effects can be neglected, considering the results of periodate treatment [9,10,18].

The above mechanisms are consistent with the experimental results from the SFA measurements reported here in that mfp-5 shows the highest adhesion, whereas mfp-3 and mfp-1 have similar adhesion to mica (figure 5).

4.3.2. SiO_2

For interactions with SiO_2, the adhesion follows the order mfp-3 > mfp-5 ≈ mfp-1 for short contact times, changing to mfp-3 > mfp-5 ≫ mfp-1 for relatively longer contacts (60 min; figure 5). The significant dependence on contact time is attributed to molecular weight and chain flexibility as discussed in §4.1 (mfp-3 > mfp-5 ≫ mfp-1). Similar to mica, bidentate hydrogen bonding by DOPA is the major contributor to mfp adhesion to SiO_2 (mfp-5 > mfp-3 ≈ mfp-1). Electrostatic interactions can play a minor role, following the order of the relative proportion of basic residues in the mfps (mfp-3 > mfp-1 ≈ mfp-5).

The adhesion energy of mfp-1 to SiO_2 was lower than that to mica, whereas the adhesion of mfp-3 and mfp-5 to SiO_2 was higher than to mica after 60 min contact. The main reason for the different adhesion trends of mfps on mica and SiO_2 could be a surface roughness issue: the root mean square (r.m.s.) roughness determined by AFM was approximately 0.2 nm for mica, whereas on SiO_2 it was 1.0 nm. For example, in the case of mfp-1, the higher roughness of SiO_2 would inhibit the smooth adhesive contact [44] between mfp-1 and SiO_2 owing to local rigidity (presence of the stiff decapeptide) of mfp-1 chains, thereby reducing the adhesion energies. On the other hand, mfp-3 and mfp-5 might adapt better to the surface roughness of SiO_2 than mfp-1 owing to their higher chain flexibility and smaller molecular weights, thereby allowing for more and stronger adhesion bonds than on mica. The adhesion energies of mfp-3 and mfp-5 show stronger contact time dependence on SiO_2 surfaces (figure 5*b*,*c*) than for the other three substrates, which implies that longer contact times lead to better conformational rearrangements of binding sites on mfp-3 and mfp-5 with the rough SiO_2 surface, as expected.

4.3.3. PMMA

For PMMA, the observed adhesion decreased as follows: mfp-3 > mfp-5 ≈ mfp-1. On the basis of the interaction mechanisms discussed in §4.2, the ability of the three mfps to provide hydrogen donors with consideration of all hydroxylation follows the order of mfp-1 > mfp-5 ≈ mfp-3, whereas the hydrophobic interactions follow the order mfp-3 > mfp-5 > mfp-1. These trends suggest that hydrophobic interactions prevail in the interactions between mfps and PMMA.

4.3.4. PS

Hydrophobic, cation–π and π–π stacking interactions can all contribute to and be important interaction mechanisms for the adhesion between mfps and PS. Considering that mfp-3 has the highest content of hydrophobic side-chains (35.5 mol%), followed by mfp-5 (29.1 mol%), and finally mfp-1 (28.6 mol%) (table 1) without adjusting for the effects of hydroxylation [13–15], the attractive hydrophobic interaction follows the order of mfp-3 > mfp-5 > mfp-1. Because the cation–π interaction strength is proportional to the amount of Lys and Arg in the mfps, which follows the order of mfp-3 (24.5 mol% Lys, Arg) > mfp-5 (22.6 mol%) > mfp-1 (20.4 mol%). π–π stacking is related to the amount of aromatic groups and roughly follows the order of mfp-3 (26.5 mol%) > mfp-5 (26.2 mol%) > mfp-1 (19.2 mol%). Therefore, after considering all the contributions above, the predicted adhesion of the mfps would follow the order of mfp-3 > mfp-5 > mfp-1, which agrees well with experimental results from SFA measurements.

It should be noted that, compared to mfp-3 and mfp-5, the relatively weak adhesion capability of mfp-1 to the different substrates is consistent with its coating as opposed to adhesive function in cuticle of byssal thread [12,18,50]. By contrast, mfp-3 is an adhesive primer for mussel adhesion and it should have underwater adhesion ability regardless of surface chemistry. Recent studies aided by SFG vibrational spectroscopy and CD strongly support the notion that mfp-3 adopts different conformations at various interfaces depending on specific chemical interactions [41–43]. Therefore, relatively stronger adhesion ability of mfp-3 to the tested substrates than mfp-1 and mfp-5 is partially due to a superior conformational adaptability of mfp-3 on the different surface chemistries.

5. Conclusions

The molecular interactions between three different kinds of *Mytilus* adhesive proteins (mfp-1, mfp-3, mfp-5) on four different substrates (mica, SiO_2, PMMA, PS) were directly measured in saline buffer using an SFA. The results provide important insights into the wet adhesion mechanisms, which were found to depend on both protein properties and substrate surface chemistry. All three proteins show adhesive versatility to both hydrophilic and hydrophobic substrates. Several interaction mechanisms are proposed, including electrostatic interaction, hydrogen bonding, hydrophobic interactions, cation–π, π–π stacking and metal-coordination. The extent to which these interactions contribute to adhesion depends on how well the critical attributes of each protein is matched to the surface tested. On the protein side, basic, aromatic and hydrophobic side-chains, the spacing between the two hydroxy groups of DOPA and chain flexibility influence the magnitude of measured mfp adhesion on all substrate. On the substrate surface side, roughness, charge, and the O–O distances of substrate surface functions are critical factors. Our results provide important insights into the design and development of biomimetic underwater adhesives and coating materials as well as anti-fouling materials.

This work was supported by an NSERC Discovery Grant Award and an NSERC RTI Grant Award (for an SFA) from the Natural Sciences and Engineering Research Council of Canada and a CSEE PoC grant (H. Zeng), the National Institutes of Health (R01 DE018468), the MRSEC Program of the National Science Foundation under award (No. DMR-1121053) (J.H.W. and J.N.I.) and the National Research Foundation of Korea Grant funded by the Korean Government (MEST) (NRF- C1ABA001- 2011-0029960) (D.S.H.).

References

1. Holten-Andersen N, Waite JH. 2008 Mussel-designed protective coatings for compliant substrates. *J. Dent. Res.* **87**, 701–709. (doi:10.1177/154405910808700808)
2. Holten-Andersen N, Fantner GE, Hohlbauch S, Waite JH, Zok FW. 2007 Protective coatings on extensible biofibres. *Nat. Mater.* **6**, 669–672. (doi:10.1038/nmat1956)
3. Harrington MJ, Masic A, Holten-Andersen N, Waite JH, Fratzl P. 2010 Iron-clad fibers: a metal-based biological strategy for hard flexible coatings. *Science* **328**, 216–220. (doi:10.1126/science.1181044)
4. Zeng H, Hwang DS, Israelachvili JN, Waite JH. 2010 Strong reversible Fe^{3+}-mediated bridging between DOPA-containing protein films in water. *Proc. Natl Acad. Sci. USA* **107**, 12 850–12 853. (doi:10.1073/pnas.1007416107)
5. Lee BP, Messersmith PB, Israelachvili JN, Waite JH. 2011 Mussel-inspired adhesives and coatings. *Annu. Rev. Mater. Res.* **41**, 99–132. (doi:10.1146/annurev-matsci-062910-100429)
6. Hennebert E, Wattiez R, Waite JH, Flammang P. 2012 Characterization of the protein fraction of the temporary adhesive secreted by the tube feet of the sea star *Asterias rubens*. *Biofouling* **28**, 289–303. (doi:10.1080/08927014.2012.672645)
7. Anderson TH, Yu J, Estrada A, Hammer MU, Waite JH, Israelachvili JN. 2010 The contribution of DOPA to substrate-peptide adhesion and internal cohesion of mussel-inspired synthetic peptide films. *Adv. Funct. Mater.* **20**, 4196–4205. (doi:10.1002/adfm.201000932)
8. Lee H, Scherer NF, Messersmith PB. 2006 Single-molecule mechanics of mussel adhesion. *Proc. Natl Acad. Sci. USA* **103**, 12 999–13 003. (doi:10.1073/pnas.0605552103)
9. Yu J, Wei W, Danner E, Israelachvili JN, Waite JH. 2011 Effects of interfacial redox in mussel adhesive protein films on mica. *Adv. Mater.* **23**, 2362–2366. (doi:10.1002/adma.201003580)
10. Yu J, Wei W, Danner E, Ashley RK, Israelachvili JN, Waite JH. 2011 Mussel protein adhesion depends on interprotein thiol-mediated redox modulation. *Nat. Chem. Biol.* **7**, 588–590. (doi:10.1038/nchembio.630)
11. Wilke P, Börner HG. 2012 Mussel-glue derived peptide-polyner conjugates to realize enzyme-activated antifouling coatings. *ACS Macro Lett.* **1**, 871–875. (doi:10.1021/mz300258m)
12. Lin Q, Gourdon D, Sun CJ, Holten-Andersen N, Anderson TH, Waite JH, Israelachvili JN. 2007 Adhesion mechanisms of the mussel foot proteins mfp-1 and mfp-3. *Proc. Natl Acad. Sci. USA* **104**, 3782–3786. (doi:10.1073/pnas.0607852104)
13. Holten-Andersen N, Zhao H, Waite JH. 2009 Stiff coatings on compliant biofibers: the cuticle of *Mytilus californianus* byssal threads. *Biochemistry* **48**, 2752–2759. (doi:10.1021/bi900018m)
14. Zhao H, Robertson NB, Jewhurst SA, Waite JH. 2006 Probing the adhesive footprints of *Mytilus californianus* byssus. *J. Biol. Chem.* **281**, 11 090–11 096. (doi:10.1074/jbc.M510792200)
15. Waite JH, Qin XX. 2001 Polyphosphoprotein from the adhesive pads of *Mytilus edulis*. *Biochemistry* **40**, 2887–2893. (doi:10.1021/bi002718x)
16. Karplus PA, Schulz GE. 1985 Prediction of chain flexibility in proteins: a tool for the selection of peptide antigens. *Naturwissenschaften* **72**, 212–213. (doi:10.1007/BF01195768)
17. Smith DK, Radivojac P, Obradovic Z, Dunker AK, Zhu G. 2003 Improved amino acid flexibility parameters. *Protein Sci.* **12**, 1060–1072. (doi:10.1110/ps.0236203)
18. Lu Q, Hwang DS, Liu Y, Zeng H. 2012 Molecular interactions of mussel protective coating protein, mcfp-1, from *Mytilus Californianus*. *Biomaterials* **33**, 1903–1911. (doi:10.1016/j.biomaterials.2011.11.021)
19. Hwang DS, Zeng H, Srivastava A, Krogstad DV, Tirrell M, Israelachvili JN, Waite JH. 2010 Viscosity and interfacial properties in a mussel-inspired adhesive coacervate. *Soft Matter.* **6**, 3232–3236. (doi:10.1039/c002632h)
20. Zeng H, Tian Y, Zhao B, Tirrell M, Israelachvili J. 2007 Transient surface patterns and instabilities at adhesive junctions of viscoelastic films. *Macromolecules* **40**, 8409–8422. (doi:10.1021/ma0712807)
21. Zeng H, Zhao BX, Tian Y, Tirrell M, Leal LG, Israelachvili JN. 2007 Transient surface patterns during adhesion and coalescence of thin liquid films. *Soft Matter.* **3**, 88–93. (doi:10.1039/b613198k)
22. Zeng H, Maeda N, Chen NH, Tirrell M, Israelachvili J. 2006 Adhesion and friction of polystyrene surfaces around Tg. *Macromolecules* **39**, 2350–2363. (doi:10.1021/ma052207o)
23. Hwang DS, Harrington MJ, Lu Q, Masic A, Zeng H, Waite H. 2012 Mussel foot protein-1 (mcfp-1) interaction with titania surfaces. *J. Mater. Chem.* **22**, 15 530–15 533. (doi:10.1039/c2jm32439c)
24. Israelachvili JN, Adams GE. 1978 Measurement of forces between 2 mica surfaces in aqueous-electrolyte solutions in range 0–100 nm. *J. Chem. Soc.-Faraday Trans.* **174**, 975–1001.
25. Helm CA, Knoll W, Israelachvili JN. 1991 Measurement of ligand receptor interactions. *Proc. Natl Acad. Sci. USA* **88**, 8169–8173. (doi:10.1073/pnas.88.18.8169)
26. Israelachvili JN *et al*. 2010 Recent advances in the surface forces apparatus (SFA) technique. *Rep. Prog. Phys.* **73**, 1–16. (doi:10.1088/0034-4885/73/3/036601)
27. Israelachvili JN, Adams GE. 1976 Direct measurement of long-range forces between 2 mica surfaces in aqueous kno3 solutions. *Nature* **262**, 773–776. (doi:10.1038/262773a0)
28. Lu Q, Wang J, Faghihnejad A, Zeng H, Liu Y. 2011 Understanding the molecular interactions of lipopolysaccharides during *E. coli* initial adhesion with a surface forces apparatus. *Soft Matter.* **7**, 9366–9379. (doi:10.1039/c1sm05554b)
29. Israelachvili JN. 1992 *Intermolecular and surface forces*, 2nd edn. London, UK: Academic Press Ltd.
30. Zhao H, Waite JH. 2006 Linking adhesive and structural proteins in the attachment plaque of *Mytilus californianus*. *J. Biol. Chem.* **281**, 26 150–26 158. (doi:10.1074/jbc.M604357200)
31. Johnson KL, Kendall K, Roberts AD. 1971 Surface energy and contact of elastic solids. *Proc. R. Soc. Lond. A* **324**, 301–313. (doi:10.1098/rspa.1971.0141)
32. Hopp TP, Woods KR. 1981 Prediction of protein antigenic determinants from amino-acid-sequences. *Proc. Natl Acad. Sci. USA* **78**, 3824–3828. (doi:10.1073/pnas.78.6.3824)
33. Nozaki Y, Tanford C. 1971 The solubility of amino acids and two glycine peptides in aqueous ethanol and dioxane solutions. *J. Biol. Chem.* **246**, 2211–2217.
34. Olivieri MP, Wollman RM, Alderfer JL. 1997 Nuclear magnetic resonance spectroscopy of mussel adhesive protein repeating peptide segment. *J. Pept. Res.* **50**, 436–442. (doi:10.1111/j.1399-3011.1997.tb01206.x)
35. Kanyalkar M, Srivastava S, Coutinho E. 2002 Conformation of a model peptide of the tandem repeat decapeptide in mussel adhesive protein by NMR and MD simulations. *Biomaterials* **23**, 389–396. (doi:10.1016/S0142-9612(01)00117-X)
36. Haemers S, van der Leeden MC, Frens G. 2005 Coil dimensions of the mussel adhesive protein Mefp-1. *Biomaterials* **26**, 1231–1236. (doi:10.1016/j.biomaterials.2004.04.032)
37. Williams JA, Le HR. 2006 Tribology and MEMSJ. *Phys. D-Appl. Phys.* **39**, R201–R214. (doi:10.1088/0022-3727/39/12/R01)
38. Jena KC, Covert PA, Hall SA, Hore DK. 2011 Absolute orientation of ester side chains on the PMMA surface. *J. Phys. Chem.* **C115**, 15 570–15 574. (doi:10.1021/jp205712c)
39. Anderson TH, Min YJ, Weirich KL, Zeng H, Fygenson D, Israelachvili JN. 2009 Formation of supported bilayers on silica substrates. *Langmuir* **25**, 6997–7005. (doi:10.1021/la900181c)
40. Rolando TE. 1998 *Solvent free adhesive*. UK: Smithers Rapra Technology.
41. Even MA, Wang J, Chen Z. 2008 Structural information of mussel adhesive protein Mefp-3 acquired at various polymer/Mefp-3 solution interfaces. *Langmuir* **24**, 5795–5801. (doi:10.1021/la800138x)
42. Le Clair SV, Nguyen K, Chen Z. 2009 Sum frequency generation studies on bioadhesion: elucidating the molecular structure of proteins at interfaces. *J. Adhes.* **85**, 484–511. (doi:10.1080/00218460902996374)
43. Hwang DS, Waite JH. 2012 Three intrinsically unstructured mussel adhesive protein, mfp-1,

mfp-2, and mfp-3: analysis by circular dichroism. *Protein Sci.* **21**, 1689–1695. (doi:10.1002/pro.2147)
44. Gay C. 2002 Stickiness: some fundamentals of adhesion. *Integr. Comp. Biol.* **42**, 1123–1126. (doi:10.1093/icb/42.6.1123)
45. Helt JM, Batteas JD. 2009 Mica surfaces: charge nucleation and wear. In *Dekker encyclopedia of nanoscience and nanotechnology*, 2nd edn. (eds SE Lyshevski, CI Contescu, K Putyera), pp. 2211–2218. New York, NY: Taylor and Francis.
46. Hwang DS, Zeng H, Lu Q, Israelachvili JN, Waite JH. 2012 Adhesion mechanism in a DOPA-deficient foot protein from green mussels. *Soft Matter.* **8**, 5640–5648. (doi:10.1039/c2sm25173f)
47. Salonen LM, Ellermann M, Diederich F. 2011 Aromatic rings in chemical and biological recognition: energetics and structures. *Angew. Chem. Int. Ed.* **50**, 4808–4842. (doi:10.1002/anie.201007560)
48. Ma JC, Dougherty DA. 1997 The cation-π interaction. *Chem. Rev.* **97**, 1303–1324. (doi:10.1021/cr9603744)
49. Waters ML. 2004 Aromatic interactions in peptides: impact on structure and function. *Biopolymers* **76**, 435–445. (doi:10.1002/bip.20144)
50. Stewart RJ, Ransom TC, Hlady V. 2011 Natural underwater adhesives. *J. Polym. Sci. Pol. Phys.* **49**, 757–771. (doi:10.1002/polb.22256)
51. Flammang P, Lambert A, Bailly P, Hennebert E. 2009 Polyphosphoprotein-containing marine adhesives. *J. Adhes.* **85**, 447–464. (doi:10.1080/00218460902996358)
52. Fukuma T, Ueda Y, Yoshioka S, Asakawa H. 2010 Atomic-scale distribution of water molecules at the mica–water interface visualized by three-dimensional scanning force microscopy. *Phys. Rev. Lett.* **104**, 01 601–01 604. (doi:10.1103/PhysRevLett.104.016101)
53. Hook F, Kasemo B, Nylander T, Fant C, Sott K, Elwing H. 2001 Variations in coupled water, viscoelastic properties, and film thickness of a Mefp-1 protein film during adsorption and cross-linking: a quartz crystal microbalance with dissipation monitoring, ellipsometry, and surface plasmon resonance study. *Anal. Chem.* **73**, 5796–5804. (doi:10.1021/ac0106501)
54. Fant C, Elwing H, Hook F. 2002 The influence of cross-linking on protein–protein interactions in a marine adhesive: the case of two byssus plaque proteins from the blue mussel. *Biomacromolecules* **3**, 732–741. (doi:10.1021/bm025506j)